

## Space-time cluster detection with cross-space-time relative risk functions

Hyeongmo Koo, Monghyeon Lee, Yongwan Chun & Daniel A. Griffith


To cite this article: Hyeongmo Koo, Monghyeon Lee, Yongwan Chun & Daniel A. Griffith (2019): Space-time cluster detection with cross-space-time relative risk functions, *Cartography and Geographic Information Science*, DOI: [10.1080/15230406.2019.1641149](https://doi.org/10.1080/15230406.2019.1641149)

To link to this article: <https://doi.org/10.1080/15230406.2019.1641149>



Published online: 29 Jul 2019.



[Submit your article to this journal](#) 







Article views: 17



[View Crossmark data](#) 

ARTICLE

## Space-time cluster detection with cross-space-time relative risk functions

Hyeongmo Koo <sup>a,b,c</sup>, Monghyeon Lee <sup>d</sup>, Yongwan Chun <sup>e</sup> and Daniel A. Griffith <sup>e</sup>

<sup>a</sup>Key Laboratory of Virtual Geographic Environment, Nanjing Normal University, Nanjing, China; <sup>b</sup>State Key Laboratory Cultivation Base of Geographical Environment Evolution, Nanjing, China; <sup>c</sup>Jiangsu Center for Collaborative Innovation in Geographical Information Resource Development and Application, Nanjing, China; <sup>d</sup>Samsung Electronics Co. Ltd., Hwasung-si, Gyeonggi-do, Korea; <sup>e</sup>School of Economic, Political and Policy Sciences, University of Texas at Dallas, Richardson, TX, USA

### ABSTRACT

Space-time kernel density estimation (STKDE) commonly is used for space-time cluster detection. But, this technique might be limited because it does not take into account an underlying population at risk for observed events. A space-time relative risk function (STRRF) can help overcome this limitation by allowing a comparison of each kernel density of observations with that of controls. This paper proposes a cross-STRRF to identify spatio-temporal locations that experience statistically significant changes in their density of events. With events organized in a space-time voxel structure, the cross-STRRF evaluates space-time patterns by comparing event occurrences at a spatial location in a previous time period with ones in its future as well as with its spatial neighbors in its contemporaneous time period. The test statistics of the cross-STRRF values in each voxel are obtained with a permutation test in which cases and controls are shuffled within each time period to maintain the space-time envelope of events. An application to assault crime incidents in the city of Plano, Texas between 2008 and 2012 illustrates that the cross-STRRF and its significance test results emphasize spatio-temporal changes in event density rather than constantly focusing on high density regions, which STKDE does.

### ARTICLE HISTORY

Received 31 January 2019  
Accepted 4 July 2019

### KEYWORDS

Space-time cluster detection; space-time kernel density estimation; space-time relative risk function; volume rendering; assault crime

## 1. Introduction

Space-time cluster detection seeks to find time and regions where events are densely located, and to statistically test whether or not the dense event pattern deviates from a random chance occurrence. Because a space-time cluster can reveal a critical and fundamental aspect of a spatio-temporal process, space-time cluster detection has been utilized as one of the basic tools in a wide range of research fields, including criminology, epidemiology, demography, regional science, and geography (e.g. Berk & MacDonald, 2009; Johnson, Bowers, & Johnson, 2008; Nakaya & Yano, 2010; Rey, Mack, & Koschinsky, 2012; Tompson & Townsley, 2010). Recently, space-time kernel density estimation (STKDE) has been utilized for space-time cluster detection, with an ability to explicitly illustrate local variations in a density of events (e.g. Brunson, Corcoran, & Higgs, 2007; Delmelle, Dony, Casas, Jia, & Tang, 2014; Nakaya & Yano, 2010). However, STKDE deals with space-time clusters as a summary of density for an entire study area at a particular time, rather than quantification of density changes over time, although the levels of event densities at a particular time and location influence their levels at their neighbors and in their future

(Rey et al., 2012). STKDE also shows only density (i.e. the number of events per area), and does not support comparisons of an observed process with a reference process (i.e. events per target) (Eck & Weisburd, 1995). For example, STKDE clusters might be an outcome of an underlying population at risk spatio-temporal process (i.e. spatial and temporal distributions of a population at risk). This weakness stimulated the development of the space-time relative risk function (STRRF) (Zhang et al., 2011), which is an extension of a spatial relative risk function (Bithell, 1990; Kelsall & Diggle, 1995a). STRRF compares kernel densities of observations (or events) and controls (i.e. events in a comparison group), and identifies space-time clusters while considering an underlying population at risk.

Finding proper controls for STRRF is not easy (Boggs, 1965), although a choice of controls plays a critical role in this type of case-control cluster analyses (Wheeler, 2007). Several space-time cluster detection methods have been developed to reflect inhomogeneous risk of cases (e.g. Mohler, Short, Brantingham, Schoenberg, & Tita, 2011; Zhuang, Ogata, & Vere-Jones, 2002), but still many methods (e.g. Kulldorff, 1997, 2001; Rogerson, 1997) largely rely on population counts in a fixed time and a spatial unit (e.g.

decennial census data). However, these population counts might lead to analysis results that deviate considerably from reality because controls constructed with these population counts assume a static and homogenous risk within spatio-temporal units for which data have been collected (e.g. annual estimates based on census tracts) (Kim & O’Kelly, 2008). In other words, controls cannot necessarily reflect a continuously varying population at risk. In addition, a fixed underlying population at risk in space and time considers spatio-temporal phenomena as occurring at a single snapshot in time, although event occurrences in the past have a great impact on future occurrences in a region (Rey et al., 2012). Furthermore, a certain type of event (e.g. assault incidents) encounters difficulty in having its underlying population at risk defined with aggregated night-time population counts (e.g. decennial census data), often requiring disaggregated micro-level data for a proper definition (Schubert, 2009). Also note that studies increasingly propose approaches to construct a more appropriate population at risk, such as Mburu and Helbich (2016), that adjust census population with commuter information (a commuter-harmonized ambient population).

This paper proposes a cross-STRRF, a modified version of STRRF (Zhang et al., 2011), in order to capture spatio-temporal locations that experience statistically significant changes in their density of events. This cross-STRRF considers the effect of past events on the occurrence of future events and on its spatial neighbors, which allows a researcher to quickly capture sudden changes in a density of events. In addition, because this cross-STRRF does not require additional data for representing an underlying population at risk, phenomena with a limited availability of population data (i.e. the control) can be seamlessly analyzed with it. The utility of this cross-STRRF is demonstrated with its application to assault crime incidents in the city of Plano, Texas during a 5 year period from 2008 to 2012. In this application, the characteristics of this cross-STRRF are illustrated, and cross-STRRF results are compared to STKDE results based on a volume rendering approach. Two different test statistics for this cross-STRRF, which include local tests for each voxel and global tests for each time period, are obtained with a permutation test, and visualized using an isosurface approach and graphs.

## 2. Literature review

Space-time cluster detection methods generally are categorized into retrospective and prospective analyses based on their use of data and corresponding continued analyses in space-time (Sonesson & Bock, 2003). Because a retrospective analysis finds space-time clusters based on an entire dataset during a single analysis (e.g. Diggle,

Chetwynd, Häggkvist, & Morris, 1995; Jacquez, 1996; Knox & Bartlett, 1964; Mantel, 1967), it is difficult to use to evaluate cluster changes over time because their results provide only a snapshot depiction (Rey et al., 2012). In addition, a retrospective analysis is unable to identify clusters at specific locations and time periods (Scholz & Lu, 2014), and, moreover, their results might be biased when the underlying population at risk is not constant over space (Paiva, Assunção, & Simões, 2015).

A prospective analysis is useful to find newly emerging and continuously changing clusters in space-time by comparing new information with prior data (Rogerson, 1997). However, the previous methods in this perspective have their own limitations. Specifically, although cumulative sum (CUSUM) statistics (Rogerson, 1997, 2001; Rogerson & Sun, 2001) are used to detect emerging space-time clusters for point phenomena (e.g. crime and disease) during specific time periods, they cannot identify the locations of these clusters. The space-time scan statistic (Kulldorff, 2001) also derived expected counts from information in a fixed time interval and a bounded enumeration unit (e.g. Gao, Guo, Liao, Webb, & Cutter, 2013; Nakaya & Yano, 2010), which yields a substantial bias in the resulting expected counts (Kim & O’Kelly, 2008).

Recent advances in prospective space-time cluster detection analyses overcome weaknesses of the aforementioned methods, and can provide efficiency in detecting spatio-temporal clusters. Specifically, a bootstrap-based surveillance model (Kim & O’Kelly, 2008) overcomes the boundary restriction of the space-time scan statistics, which raises the issue of population at risk data. A windowed nearest neighbor approach (Pei, Zhou, Zhu, Li, & Qin, 2010) adopts the concept of the windowed  $k^{\text{th}}$  nearest distance in order to avoid subjectivity in defining scanning windows in a space-time scan statistic. However, this approach is unable to distinguish a space-time cluster from a random pattern due to its lack of including the population at risk. Recently, prospective surveillance methods have been posited that include a cumulative surface based on local Knox scores to identify emerging clusters of events (Paiva et al., 2015). However, determining an optimal bandwidth for a cumulative surface and its effects need to be further investigated because the shape of the cumulative surface highly depends on the employed bandwidth. In addition, Rey et al. (2012) introduce new exploratory methods for space-time analysis, which are a conditional spatial Markov chain and its extension with a joint spatial Markov chain. Their methods quantify the dynamics of events in space and time by relating the probabilities of events at each location in a future period to those in a preceding period, and also by considering the impact of each location on its spatial neighbors.

Although space-time analyses increasingly have been appearing in the literature during the last two decades (e.g. An et al., 2015; Hu, Griffith, & Chun, 2018), many studies still are limited in their evaluations of cluster changes in space and time for a number of reasons. First, all retrospective analyses and some prospective analyses (e.g. Rey et al., 2012; Rogerson & Sun, 2001) are not able to specify locations and time periods where and when space-time clusters occur. Second, because some space-time cluster detection methods (e.g. Nakaya & Yano, 2010; Pei et al., 2010) are limited in their consideration of population at risk, their space-time clustering outcomes can be differentiated from a random pattern due to chance under a homogenous assumption about population. Third, population at risk usually is derived from data that are collected in a bounded enumeration unit in a fixed time interval (e.g. Kulldorff, 1997, 2001; Rogerson, 1997). Thus, population at risk might deviate considerably from reality.

Visualizing space-time clusters is also a challenge. While the concept of the space-time cube that originated in time-geography diagrams (Hägerstrand, 1970) is useful for a visualization of continuous spatio-temporal phenomena, representing clusters with voxels in the space-time cube still is challenging due to its four-dimensional space nature: geographic space, time, and its value. The isosurface approach is one of the effective ways to visualize values at voxels (Brunsdon et al., 2007). Specifically, this approach connects voxels with a cutoff value, which is similar to the isoline in a two-dimensional space. However, the cutoff value mainly depends on an arbitrary decision by researchers (McLafferty, Williamson, & McGuire, 2000), and a representation of overlaid isosurfaces with several cutoff values is difficult to do because the insides of isosurfaces cannot be displayed. Recently, a volume rendering approach successfully provided intuitive representations of cluster changes over time and space in a space-time cube (e.g. Delmelle et al., 2014; Nakaya & Yano, 2010). This volume rendering approach makes the value of opacity at each voxel high for low values, and, in contrast, low for high values, so that voxels with high values are visible as a solid volume through completely or partially transparent voxels (Nakaya & Yano, 2010).

### 3. Methods

#### 3.1 Space-time kernel density estimation and space-time relative risk function

This section begins with a review of STKDE and STRRF that provides the fundamental components for the cross-STRRF. Kernel density estimation (KDE) is a commonly used method to estimate the density of events in space (Silverman, 1986), which can be utilized

to summarize and visualize spatial patterns of events and clusters (e.g. Chainey & Ratcliffe, 2005). Density at the point  $(x, y)$  can be estimated with

$$\hat{f}(x, y) = \frac{1}{nh_1^2} \sum_{i=1}^n k_1\left(\frac{x-x_i}{h_1}, \frac{y-y_i}{h_1}\right), \quad (1)$$

where  $k_1(\cdot, \cdot)$  is a probability density function,  $h_1$  is the bandwidth of space, and  $n$  is the number of events. STKDE results from an addition of the temporal dimension to KDE under the first-order separable assumption between space and time (Chun, 2014; Gabriel, Rowlingson, & Diggle, 2013; Griffith, 2012; Schoenberg, 2004).

$$\hat{f}(x, y, t) = m(x, y) \cdot \mu(t), \quad (2)$$

where  $m(x, y)$  and  $\mu(t)$  denote spatial and temporal density, respectively. Under the assumption, STKDE can be estimated with (Brunsdon et al., 2007; Delmelle et al., 2014; Nakaya & Yano, 2010)

$$\hat{f}(x, y, t) = \frac{1}{nh_s^2 h_t} \sum_{i=1}^n k_s\left(\frac{x-x_i}{h_s}, \frac{y-y_i}{h_s}\right) k_t\left(\frac{t-t_i}{h_t}\right), \quad (3)$$

where  $h_s$  and  $h_t$  are the spatial and temporal bandwidths, respectively, and  $k_s(\cdot, \cdot)$  and  $k_t(\cdot)$  are the spatial and temporal kernel density functions, respectively.

STKDE is a technique for generating the density distribution of events rather than detecting clustering (Pei et al., 2010). If an underlying population at risk for spatio-temporal events is uniformly distributed across an entire study area, a simple STKDE map is a useful way to find the clusters of events. However, in most empirical cases, the population at risk usually does not conform to a uniform distribution. That is, an individual point has its corresponding risk that varies across spatio-temporal locations. For example, in the context of a spatial domain only, the number of residential burglary incidents in a given spatial unit is closely related to the number of households in that unit. Thus, the densities of both cases and controls are estimated using KDE in order to find significant clusters by excluding clusters occurring by random chance. The ratios of case densities to control densities are regarded as a “relative risk function (RRF)” (Bithell, 1990). A RRF can be extended to a STRRF by adding a temporal domain, which is represented by the ratio of the following case-to-control STKDE equation (Zhang et al., 2011):

$$r(x, y, t) = \frac{\hat{f}_{case}(x, y, t)}{\hat{g}_{control}(x, y, t)}. \quad (4)$$

Using the logarithm of  $r(x, y, t)$  is recommended in order to reduce the effects of extreme values as well as to

improve the symmetry of the risk function (Kelsall & Diggle, 1995a, 1995b; Zhang et al., 2011). The following logarithm form of STRRF is used in this article:

$$\rho(x, y, t) = \ln \frac{\hat{f}_{case}(x, y, t)}{\hat{g}_{control}(x, y, t)}. \quad (5)$$

### 3.2 The cross space-time relative risk function

Selection of a proper control function plays an important role in STRRF analysis, although this selection may be difficult in an empirical analysis because of a lack of data (e.g. daytime population and disaggregated data). However, the cross-STRRF employs a control function based on Markov chain theory for analyzing the dynamics of events in space and time, rather than using an additional dataset for a control function. In certain types of events (e.g. crime incidents), a strong effect of past events on a future event occurrence has been recognized from related theories [e.g. routine activities (Cohen & Felson, 1979), rational choice theories (Clarke & Cornish, 1985)], and the analyses of crime event repeats (e.g. Ratcliffe & Rengert, 2008; Short, D'Orsogna, Brantingham, & Tita, 2009). Specifically, analyzing residential burglary incidents, Rey et al. (2012) also adopt Markov chain theory to show a strong relationship between the probability of future event occurrences and the prevalence of events in neighboring locations at a current period. In this paper, a discrete first-order Markov chain is used, which assumes that the conditional probability of the present point ( $t$ ) is only determined by the most recent past point ( $t - 1$ ), not all of the preceding points in time ( $1, \dots, t - 1$ ) (Haining, 2003):

$$\begin{aligned} \text{Prob}\{Z(t) = z(t) | Z(1) = z(1), \dots, Z(t-1) = z(t-1)\} \\ = \text{Prob}\{Z(t) = z(t) | Z(t-1) = z(t-1)\}. \end{aligned}$$

For the cross-STRRF, the control and case functions [Equation (5)] are determined by Markov chain theory. Specifically, this procedure is implemented by repeatedly dividing STKDE into case and control functions based on reference times. In other words, the control function of the cross-STRRF is constructed with preceding events from a reference time point, and the case function consists of event points that occurred after the reference time point (Figure 1). Accordingly, the components of the cross-STRRF can be represented as

$$\begin{aligned} \hat{f}_{case}(x, y, t) = \frac{1}{nh_s^2 h_t} \sum_{i=1}^n k_s \left( \frac{x - x_i}{h_s}, \frac{y - y_i}{h_s} \right) k_t \left( \frac{t - t_i}{h_t} \right), \\ \text{where } t_i \geq t, \end{aligned} \quad (6)$$

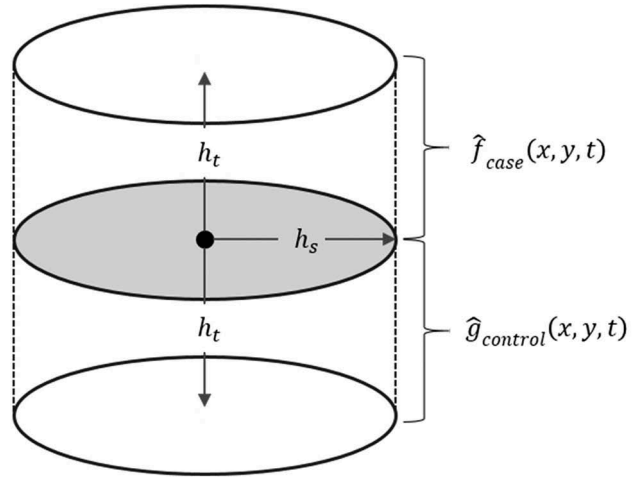


Figure 1. Components of the cross space-time risk function.

and

$$\begin{aligned} \hat{g}_{control}(x, y, t) = \frac{1}{nh_s^2 h_t} \sum_{i=1}^n k_s \left( \frac{x - x_i}{h_s}, \frac{y - y_i}{h_s} \right) k_t \left( \frac{t - t_i}{h_t} \right), \\ \text{where } t_i < t. \end{aligned} \quad (7)$$

From these components, the cross-STRRF considers the impact of events on a certain point from not only a preceding period, but also its neighbors.

Figure 3 illustrates the difference between STKDE and the cross-STRRF with a simple synthetic example (Figure 2). For simplicity, all cell sizes are the same, namely one, and all events in each cell are summarized with the same weight without considering distance (i.e. a uniform density function). The result of using STKDE for the current events (Figure 3(a)) represents the event density (e.g. the numbers in the cells) without considering population at risk and the effect of past events. Thus, STKDE detects cells i and iv as high and low clusters, respectively. Meanwhile, the cross-STRRF compares the density of past events (Figure 2(a)) and current events (Figure 2(b)) in the logarithm form [Equations (6) and (7), respectively], which captures changes in the densities. Therefore, the cross-STRRF captures increasing and decreasing densities in cells ii and iii (Figure 3(b)). Furthermore, this approach accounts for events along with temporally continuous influences and a geographically neighboring effect, rather than dealing with clusters of events as a separated phenomenon at a point in time like STKDE and STRRF do.

### 3.3 Bandwidths, kernel function selection, and a significance test

The cross-STRRF has two important components that are also necessary for the STRRF and STKDE: selection

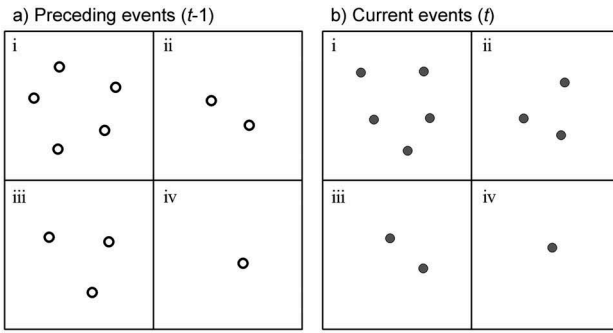


Figure 2. The synthetic example.

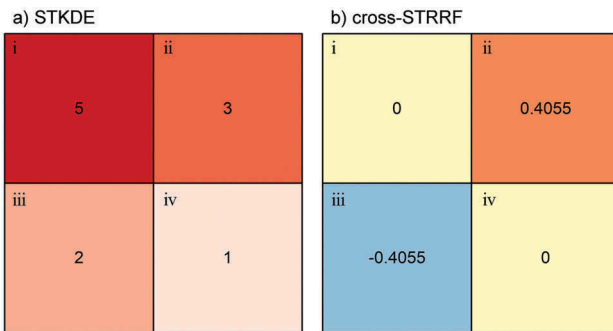


Figure 3. The example results of the spatio-temporal density and the cross space-time relative risk functions.

of a kernel function, and spatio-temporal bandwidths. First, a bandwidth is a critical component in KDE and its variants because the degree of smoothness in an estimated density surface primarily depends on the size of a bandwidth (Silverman, 1986). Usually, a large bandwidth leads to a smooth surface, in which important spatio-temporal fluctuations in space and time might not be detected (Nakaya & Yano, 2010). In contrast, a small bandwidth likely results in a less smooth surface (i.e. a spiky surface), where prominent patterns of events are difficult to illustrate. Here, the effects of two optimal bandwidths, which are generated from a plug-in method (Scott, 1992) and a space-time  $K$ -function (Delmelle, Casas, & Barto, 2011), are compared based on the results of STKDE and the cross-STRRF. Specifically, the Scott's plug-in estimation finds optimal bandwidths that minimize the asymptotic mean integrated squared error from an orthogonal multivariate normal distribution assumption (Nakaya & Yano, 2010). The plug-in estimation is given as

$$\hat{h}_i = n^{-1/(3+d)} \hat{\sigma}_i, \quad (8)$$

where  $\hat{\sigma}_i$  is the standard deviation in the  $i^{\text{th}}$  dimension, and  $d$  is the number of dimensions. The space-time Ripley's  $K$ -function (Diggle et al., 1995) evaluates the presence of space-time clusters at particular spatio-

temporal scales. The spatio-temporal scale shows the clusters of events that can be used as candidates for optimal bandwidths of STKDE (e.g. Delmelle et al., 2014).

Second, a proper choice of a kernel function is required for the cross-STRRF and STKDE. Although the choice of a kernel function is less critical than the size of a bandwidth (Kelsall & Diggle, 1995a; Silverman, 1986), the standard Gaussian density function tends to produce more smooth general KDE surfaces than other widely used kernel functions (e.g. quadratic, uniform, triangular, and negative exponential density functions) (Borruso, 2008; Levine, 2010). Thus, this analysis uses the Gaussian density function to highlight more general trend. With the independence assumption between space and time (e.g. Brunsdon et al., 2007), the kernel function in Equations (6) and (7) can be represented as a product of three univariate Gaussian kernel functions, each of which may be defined as follows:

$$k(w) = \begin{cases} \frac{1}{\sqrt{2\pi}} \exp\left(-\frac{w^2}{2}\right), & w^2 < 1 \\ 0, & \text{otherwise} \end{cases} \quad (8)$$

In this kernel function, the contribution to the density estimation at a certain point depends on the closeness of each event to that point (Bailey & Gatrell, 1995). In other words, close events from an estimated point have larger impacts than distant ones. With a kernel function, this approach may overcome the weakness of space-time scan statistics that distance and time decay effects are not reflected.

Finally, the cross-STRRF requires an edge correction to reduce bias around the boundaries of a study area and time. At the boundaries of a study area, the densities of the cross-STRRF are underestimated, because they are calculated with the same bandwidths as the interior of the study area. Thus, density values nearby the boundaries should be inflated with an edge correction. For a spatial dimension, this paper utilizes Berman and Diggle (1989)'s edge correction method, which inflates density values nearby the boundaries based on the magnitude of the intersection between a kernel and the study area. For a temporal dimension, more events in a temporally buffered area around the temporal extent are collected (Bailey & Gatrell, 1995).

A significance test for the cross-STRRF can be constructed with a permutation test because its statistical distribution cannot be directly derived due to its strong spatial autocorrelation among estimated KDE values (McLafferty et al., 2000). In detail, the permutation method shuffles cases and controls in each time period, which ensures that the spatial and temporal envelope of the events remains the same as in the original dataset

(Guo, 2010). Then, the exact same estimation procedure is applied to this simulated dataset. In this application, the permutation step is repeated 999 times to obtain the reference distribution of the cross-STRRF values at each voxel employing a Monte Carlo method (Dwass, 1957). The overall procedure for the permutation test is similar to that outlined by Kulldorff, Heffernan, Hartman, Assunção, and Mostashari (2005). In addition to the test of the cross-STRRF values at each voxel, the permutation result can be used for a test for global clustering during each time period. The global clustering test evaluates whether or not the observed values are consistent with the underlying population at risk across a study region (Bivand, Pebesma, & Gómez-Rubio, 2008). That is, the test statistic is a sum of squared values of the cross-STRRF across an entire study area in each time period (Kelsall & Diggle, 1995a; Wheeler, 2007), where the significance of the test statistic for global clustering also is evaluated based on Monte Carlo methods (Kelsall & Diggle, 1995b).

In summary, the cross-STRRF can be defined using Equations (6) and (7), where the standard Gaussian function is used for the kernel functions,  $k_s(\cdot)$  and  $k_t(\cdot)$ . The cross-STRRF is evaluated with the two different types of bandwidths generated from a plug-in method and a space-time  $K$ -function. The significance tests for local and global clustering in the cross-STRRF are conducted with a permutation test. Finally, Berman and Diggle (1989) buffering methods are applied for spatial and temporal edge correction methods, respectively.

#### 4. An application

Crime incidents in the city of Plano, Texas from 2008 to 2012 (5 years) are analyzed with STKDE and the cross-STRRF. The city of Plano is located in the north-eastern part of the Dallas-Fort Worth-Arlington

metropolitan statistical area, and has approximately 260,000 residents according to the United States 2010 decennial census. The crime incidents data were obtained from the City of Plano Police Department. These data contain occurrence time and are organized with a time aggregation at the hour level for computational simplicity. Among various types of crime, assault crime incidents are analyzed because night time population information (i.e. census data) may not accurately reflect an underlying population at risk for assault crime (Waller, Zhu, Gotway, Gorman, & Gruenewald, 2007). Furthermore, assault crime incidents often are more highly correlated with particular locations, such as pub leisure zones and shopping streets (Nelson, Bromley, & Thomas, 2001), than with night time population. The sample R code for the cross-STRRF and all direct volume rendering figures in the Voxler environment (Golden Software, Colorado) are available online (<https://github.com/hyeongmokoo/crossSTRRF>).

This dataset contains 9,301 assault crime incidents during the 5-year period from 1 January 2008, to 31 December 2012. Figure 4 portrays the distribution of assault crime incidents in the spatial and temporal dimensions. The density surface of assault crime incidents, generated by KDE with a 4,100-foot bandwidth, presents the spatial pattern of the assault incidents during the entire period. Four clusters, which have high crime densities greater than 300 assault incidents per square miles, are arbitrarily extracted to help understand the spatial distribution of assault crime incidents (Figure 4(a)). The four assault crime clusters generally coincide with high-activity areas (Sherman, Gartin, & Buerger, 1989). Specifically, in Figure 4(a), Cluster I is found in downtown Plano, and Clusters II, III, and IV are located in major commercial districts. The geographic locations of these four clusters are utilized to compare STKDE and the cross-STRRF

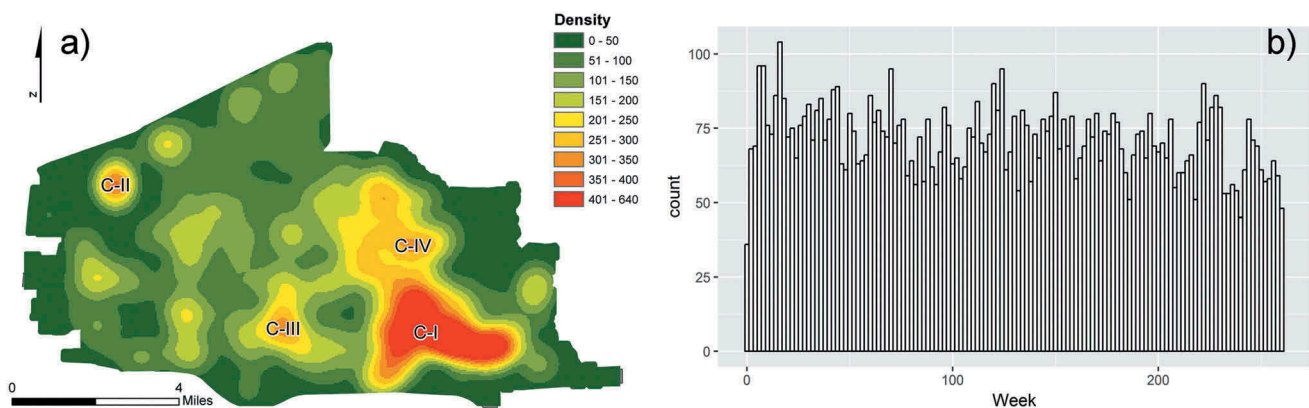


**Figure 4.** Space and time distributions of assault incidents in the city of Plano, (a) KDE for a spatial distribution (the number of incidents per square mile), and (b) a time series incidents histogram with two-week intervals.

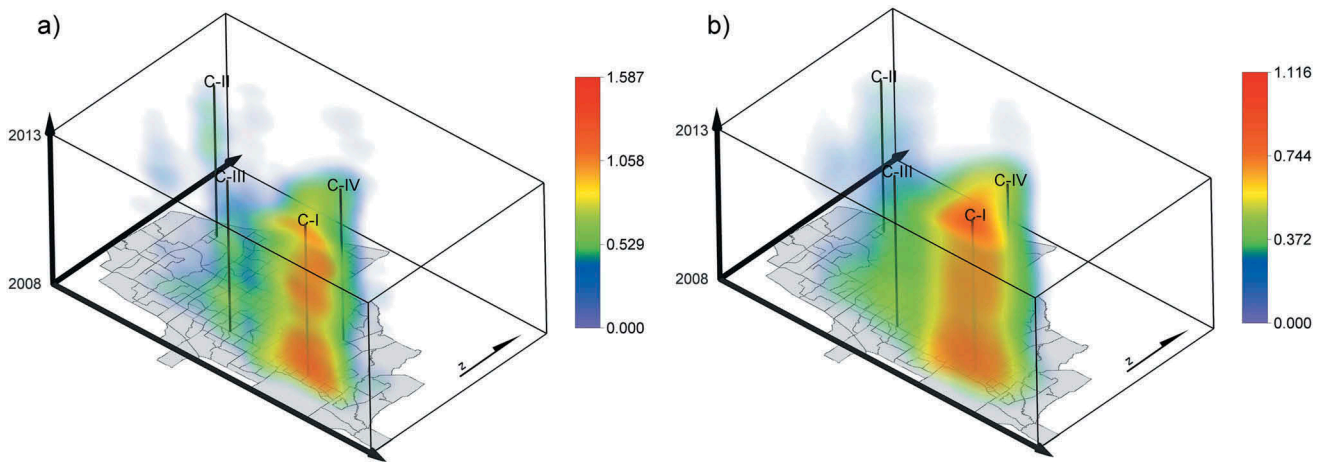


**Figure 5.** The spatio-temporal density of assault incidents (the number of incidents per square mile per week). (a) from Scott's plug-in and (b) from a space-time  $K$ -function.

results later in this section. [Figure 4\(b\)](#) shows frequencies of assault incidents aggregated into two-week intervals. Overall, the frequency of incidents decreases exhibiting local variation.

[Figure 5](#) shows the direct volume rendering of STKDE, where each voxel has different opacity and optical colors based on its density value (Nakaya & Yano, 2010), which provides an instinctive display of the density changes in the space-time cube. Each voxel has the spatial resolution of 300-by-300 feet and the temporal resolution of 14 days; 4,259,840 voxels are used. In addition, four vertical lines are inserted to represent the centers of the clusters (see [Figure 4\(a\)](#)). These results are generated with two different types of optimal bandwidth selection methods: (1) Scott's plug-in estimates, and (2) a space-time  $K$ -function with spatial and temporal bandwidths. The estimated values are  $x = 3,378$  feet,  $y = 2,044$  feet, and 115 days for (1), and  $x$  and  $y = 4,100$  feet and 239 days for (2). In the result of the space-time  $K$ -function, the strongest clustering, which shows the largest difference between the space-time  $K$ -function and the product of separate spatial and temporal  $K$ -functions (Delmelle et al., 2011), is found at spatial and temporal scales with 25,300 feet and 85 days. However, the optimal bandwidths are chosen from the second strongest clustering, because the spatial bandwidth from the strongest clustering is too large to capture local variations.

The density distribution generated from the space-time  $K$ -function ([Figure 5\(b\)](#)) exhibits an over smoothed surface compared with results with the plug-in estimate. This outcome shows only one large cluster at the location of Cluster I, which coincides with the downtown. In contrast, the volume rendering image based on the plug-in estimate ([Figure 5\(a\)](#)) displays more detailed changes in the crime density distribution. Specifically,

the geographical region of Cluster I shows a high assault incidents density throughout across all time periods, although the density values show a small variation in the temporal dimension. This result indicates that the density of assault incidents is consistently high in the downtown area. In contrast, the other clusters, especially Clusters II and III, have short temporal durations. That is, Cluster III appears at the bottom of the space-time cube (i.e. high density in 2008), and Cluster II appears at the top of the cube (i.e. high density in 2012).

[Figure 6\(a,b\)](#) present the cross-STRRF results in volume rendering images. The cross-STRRF uses the same bandwidth for the case and control kernel functions in order to equally cover spatial and temporal extents in the numerator and denominator of the ratio like a general STRRF does (Wheeler, 2007). As for the STKDE, the cross-STRRF is conducted with plug-in estimates and a space-time  $K$ -function. The computing times of the cross-STRRF are 36.25 and 38.84 seconds with the estimated bandwidth of Scott's plug-in and a space-time  $K$ -function, respectively. An Intel i5-7500 processor with 3.40GHz of clock rate was used for this calculation. The computing time can vary with the number of voxels and the size of bandwidths (Delmelle et al., 2014). Overall, the volume rendering image of the cross-STRRF obtained with the plug-in estimate ([Figure 6\(a\)](#)) is less smoothed than the one obtained with the space-time  $K$ -function ([Figure 6\(b\)](#)). The spatio-temporal pattern of clustering changes may not be clearly displayed in [Figure 6\(a\)](#). In contrast, [Figure 6\(b\)](#) has a more smoothed surface, which might help to foster an understanding of general spatial and temporal dynamics of the crime incident patterns.

Explicitly, the cross-STRRF result with the space-time  $K$ -function bandwidth ([Figure 6\(b\)](#)) reveals a remarkable



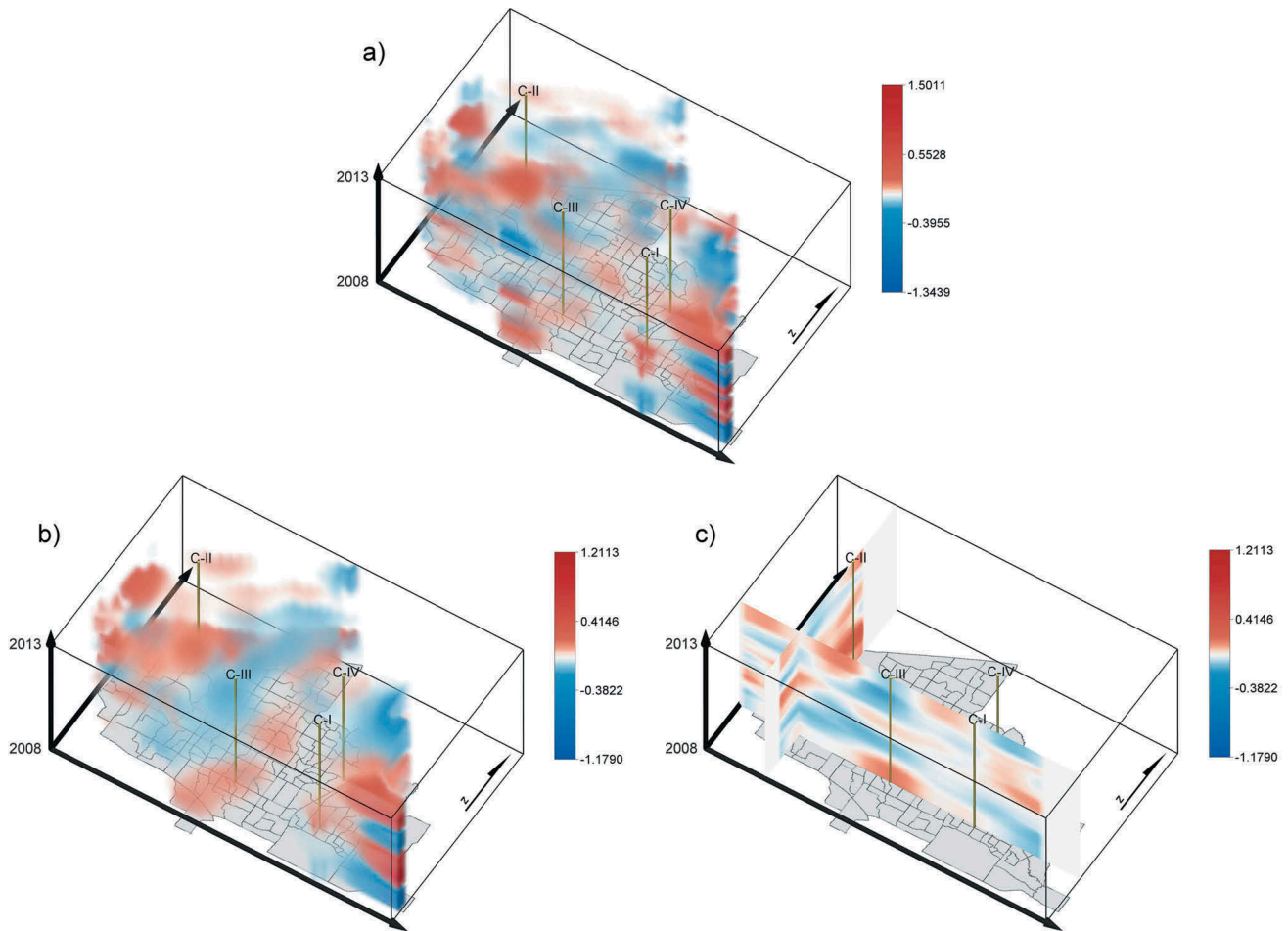


**Figure 6.** The cross space-time relative risk functions of assault incidents. (a) from Scott's plug-in, (b) from a space-time  $K$ -function, and (c) based upon slices of a space-time  $K$ -function.

characteristic of the cross-STRRF that captures spatio-temporal locations in dramatic event density changes. Figure 6(c) is presented to assist the understanding of the characteristics of the cross-STRRF by adding two vertical planes to the space-time  $K$ -function result (Figure 6(c)), where these planes intersect each other at the centers of Clusters II and III. Specifically, although Cluster I is prominent in the result of the STKDE, the cross-STRRF does not focus on this constantly high density region. Instead, the cross-STRRF emphasizes the spatio-temporal dynamics of the incidents density. For example, the cross-STRRF results (Figure 6(b,c)) capture an increasing incidents density in the Cluster III region (i.e. the south-central part of the city) during early 2008, and a decreasing incidents density during late 2012, which would not be identified by the STKDE. In contrast, the Cluster II region (i.e. the north-western part of the city) clearly shows an increasing density pattern when compared to the preceding period from October 2012 to December 2012.

A significance test is constructed for the cross-STRRF result with the space-time  $K$ -function bandwidth (see Figure 6(b)). Figure 7(a,b) show significant changes in assault incidents at the voxel level, and the probability values of the global clustering test at each time period, respectively. In detail, Figure 7(a) displays significant isosurfaces for the incident dynamics at the 5% significance level, where the increasing (red) and decreasing (blue) densities of assault incidents have been compared with their corresponding previous densities. The significant isosurfaces help to exhibit considerable changes in the incidents density in present and near future periods. For example, the Cluster I region (see Figure 5) has no significant isosurface because this region has a continuously high density of incidents. In contrast, Figure 5(a) clearly captures a significantly increasing isosurface in the Cluster IV region in late 2011, and another in the Cluster II region in late 2012. The Cluster III region shows an alternating appearance of increasing and decreasing isosurfaces. That is, the significant increasing

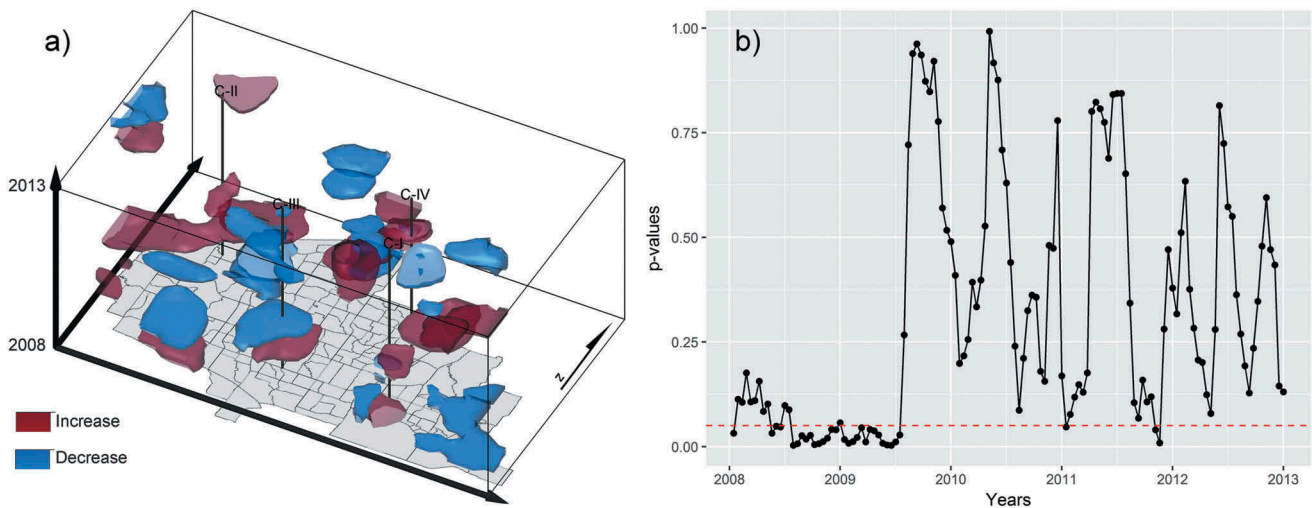


**Figure 7.** The significant clusters of the cross-space-time relative functions for assault incidents. (a) local clustering by space and time, and (b) global clustering by time period.

isosurface in early 2008 is followed by a significant decreasing isosurface in this region. Then, in late 2012, a significant decrease in density of assault incidents appears again. Another observation appears in the south-east of the study area. Figure 6 shows that opposite values of the cross-STRRF are observed along the temporal axis in this region, which is suspected to happen due to an over-inflation by edge correction. However, significant isosurfaces exist only in early 2008 (Figure 5(a)).

Figure 7(b) shows the  $p$ -values of the test statistic for global dynamics in each time period that provides a summary measure for spatial dynamics in a given time period. A significant  $p$ -value means that the densities of the crime incidents in a future period do remain similar with a preceding period across the study area in a given period. In Figure 7(b), the significant dynamics of the density mainly appear around between May 2008 and July 2009. That is, in this period, the city of Plano has experienced dramatic changes in the spatial distribution of the assault crime density. For example, in May 2008, a sharp decreasing pattern of the crime density is mainly found around the Cluster II region (Figure 6(a)), and, in contrast, a dramatic increasing pattern is detected around Cluster III from August 2008 to November 2008. In addition, from May 2009 to July 2009, increasing and decreasing patterns of the density are founded in northwest of the city and the Cluster III region, respectively. Also, the  $p$ -value less than 0.05 in November 2011 is due to an increasing pattern of the density around the Cluster IV region. In contrast, other time periods generally have densities consistent with their corresponding preceding periods, except for the time period from May 2008 to July 2009.

## 5. Conclusion

This paper proposes the cross-STRRF by reexpressing the general STKDE in terms of case and control functions in order to detect spatio-temporal regions that experience dramatic changes in their density of events. This paper also presents a comparison between STKDE and the cross-STRRF with an application of assault incidents in the city of Plano, Texas. The application results show that the cross-STRRF has three advantageous characteristics compared to the STKDE and the general STRRF, which is a main contribution of this paper to the literature. First, the cross-STRRF emphasizes the spatio-temporal dynamics of events by comparing the probabilities of these events at each location and its neighbors in a future period with those in a preceding period. However, the STKDE accounts for clusters of events as a separate phenomenon at a point in time without considering spatio-temporally continuous effects of events. Second, unlike STRRF, the cross-STRRF does not require an additional dataset for the population at risk because it directly compares the density of events in a future period to those in a preceding period. Thus, this characteristic can help the cross-STRRF easily apply to various types of point events. Furthermore, the cross-STRRF can avoid a potential error that comes from the assumption of a constant population at risk within a given spatio-temporal unit when using common census data for a fixed time interval with a bounded enumeration unit as the population at risk. Third, the test statistics provide a summary of the cross-STRRF, which promotes an intuitive understanding of the results. Specifically, results from the local test help to find and display only the significant changes

in event densities of spatio-temporal regions, whereas results from the global test in each time period provide summary measures for spatial dynamics over time.

Some limitations to this research are worth addressing in future studies. First, because the result of the cross-STRRF is calculated in a predetermined size of voxels, the variation within a voxel cannot be identified. The small size of a voxel is preferred for detailed representation, but it might require extremely intensive computation. Thus, determining an optimal voxel size for the presentation and calculation of the cross-STRRF is necessary, giving consideration to the size of a study area and the distribution of events. Second, similar to KDE and STKDE, the smoothness of cross-STRRF surfaces primarily is determined by the sizes of spatial and temporal bandwidths. That is, results can be dramatically altered by changing the sizes of the bandwidths. Although this paper adopts the well-known optimal bandwidth selection methods for the cross-STRRF, further investigation is necessary to examine the impact of bandwidth size on a cross-STRRF result. Third, the spatio-temporal densities in both STKDE and the cross-STRRF are derived under the first-order separable assumption between space and time dimensions. This separable assumption has been utilized in space-time modeling in the literature (e.g. Delmelle et al., 2014; Nakaya & Yano, 2010; Porter & Reich, 2012). However, an approach to accommodate dependence in a space-time structure (i.e. interaction between space and time components) need to be further investigated in future research (e.g. Celik, Shekhar, Rogers, & Shine, 2008; Gabriel et al., 2013; Griffith, 2012; Knorr-Held, 2000). Finally, the cross-STRRF could be further extended by using network-based distances instead of Euclidean distances (Borruso, 2008; Okabe, Satoh, & Sugihara, 2009).

## Disclosure statement

No potential conflict of interest was reported by the authors.

## Funding

This work was partially supported by the NSF for Excellent Young Scholars of China [41622108].

## ORCID

Hyeongmo Koo  <http://orcid.org/0000-0002-5446-1668>  
 Monghyeon Lee  <http://orcid.org/0000-0002-5778-5967>  
 Yongwan Chun  <http://orcid.org/0000-0002-4957-1379>  
 Daniel A. Griffith  <http://orcid.org/0000-0001-5125-6450>

## References

- An, L., Tsou, M.-H., Crook, S. E. S., Chun, Y., Spitzberg, B., Gawron, J. M., & Gupta, D. K. (2015). Space-time analysis: Concepts, quantitative methods, and future directions. *Annals of the Association of American Geographers*, 105(5), 891–914. doi: 10.1080/00045608.2015.1064510
- Bailey, T. C., & Gatrell, A. C. (1995). *Interactive spatial data analysis*. Harlow, UK: Longman Scientific & Technical.
- Berk, R., & MacDonald, J. (2009). The dynamics of crime regimes. *Criminology*, 47(3), 971–1008. doi: 10.1111/j.1745-9125.2009.00161.x
- Berman, M., & Diggle, P. (1989). Estimating weighted integrals of the second-order intensity of a spatial point process. *Journal of the Royal Statistical Society. Series B (methodological)*, 51(1), 81–92. doi: 10.1111/j.2517-6161.1989.tb01750.x
- Bithell, J. F. (1990). An application of density estimation to geographical epidemiology. *Statistics in Medicine*, 9, 691–701. doi: 10.1002/sim.4780090616
- Bivand, R., Pebesma, E., & Gómez-Rubio, V. (2008). *Applied spatial data analysis with R*. New York: Springer. doi: 10.1007/978-1-4614-7618-4
- Boggs, S. L. (1965). Urban crime patterns. *American Sociological Review*, 30(6), 899–908. doi: 10.2307/2090968
- Borruso, G. (2008). Network density estimation: A GIS approach for analysing point patterns in a network space. *Transactions in GIS*, 12(3), 377–402. doi: 10.1111/j.1467-9671.2008.01107.x
- Brunsdon, C., Corcoran, J., & Higgs, G. (2007). Visualising space and time in crime patterns: A comparison of methods. *Computers, Environment and Urban Systems*, 31(1), 52–75. doi: 10.1016/j.compenvurbsys.2005.07.009
- Celik, M., Shekhar, S., Rogers, J. P., & Shine, J. A. (2008). Mixed-drove spatiotemporal co-occurrence pattern mining. *IEEE Transactions on Knowledge and Data Engineering*, 20(10), 1322–1335. doi: 10.1109/tkde.2008.97
- Chainey, S., & Ratcliffe, J. (2005). *GIS and crime mapping*. London: Wiley. doi: 10.1002/9781118685181
- Chun, Y. (2014). Analyzing space-time crime incidents using eigenvector spatial filtering: An application to vehicle burglary. *Geographical Analysis*, 46(2), 165–184. doi: 10.1111/gean.12034
- Clarke, R. V., & Cornish, D. B. (1985). Modeling offenders' decisions: A framework for research and policy. *Crime Justice*, 6, 147–185. doi: 10.1086/449106
- Cohen, L. E., & Felson, M. (1979). Social change and crime rate trends: A routine activity approach. *American Sociological Review*, 44(4), 588–608. doi: 10.2307/2094589
- Delmelle, E., Delmelle, E. C., Casas, I., & Barto, T. (2011). H. E.L.P: A GIS-based health exploratory analysis tool for practitioners. *Applied Spatial Analysis and Policy*, 4(2), 113–137. doi: 10.1007/s12061-010-9048-2
- Delmelle, E., Dony, C., Casas, I., Jia, M., & Tang, W. (2014). Visualizing the impact of space-time uncertainties on dengue fever patterns. *International Journal of Geographical Information Science*, 28(5), 1107–1127. doi: 10.1080/13658816.2013.871285
- Diggle, P., Chetwynd, A. G., Häggkvist, R., & Morris, S. E. (1995). Second-order analysis of space-time clustering. *Statistical Methods in Medical Research*, 4(2), 124–136. doi: 10.1177/096228029500400203

- Dwass, M. (1957). Modified randomization test for non-parametric hypotheses. *The Annals of Mathematical Statistics*, 28(1), 181–187. doi: [10.1214/aoms/1177707045](https://doi.org/10.1214/aoms/1177707045)
- Eck, J. E., & Weisburd, D. L. (1995). Crime places in crime theory. In J. E. Eck & D. L. Weisburd (Eds.), *Crime and place*. Monsey, NY: Criminal Justice Press. doi: [10.1086/229477](https://doi.org/10.1086/229477)
- Gabriel, E., Rowlingson, B., & Diggle, P. P. J. P. (2013). Stpp: An R package for plotting, simulating and analysing spatio-temporal point patterns. *Journal of Statistical Software*, 53(2), 1–29. doi: [10.18637/jss.v053.i02](https://doi.org/10.18637/jss.v053.i02)
- Gao, P., Guo, D., Liao, K., Webb, J. J., & Cutter, S. L. (2013). Early detection of terrorism outbreaks using prospective space-time scan statistics. *Professional Geographer*, 65(4), 676–691. doi: [10.1080/00330124.2012.724348](https://doi.org/10.1080/00330124.2012.724348)
- Griffith, D. A. (2012). Space, time, and space-time eigenvector filter specifications that account for autocorrelation. *Estadística Española*, 54(177), 7–34.
- Guo, D. (2010). Local entropy map: A nonparametric approach to detecting spatially varying multivariate relationships. *International Journal of Geographical Information Science*, 24(9), 1367–1389. doi: [10.1080/13658811003619143](https://doi.org/10.1080/13658811003619143)
- Hägerstrand, T. (1970). What about people in regional science. *Papers in Regional Science*, 24(1), 7–24. doi: [10.1111/j.1435-5597.1970.tb01464.x](https://doi.org/10.1111/j.1435-5597.1970.tb01464.x)
- Haining, R. (2003). *Spatial data analysis theory and practice*. Cambridge: Cambridge University Press. doi: [10.1017/cbo9780511754944](https://doi.org/10.1017/cbo9780511754944)
- Hu, L., Griffith, D. A., & Chun, Y. (2018). Space-time statistical insights about geographic variation in lung cancer incidence rates: Florida, 2000–2011. *International Journal of Environmental Research and Public Health*, 15(11), 2406. doi: [10.3390/ijerph15112406](https://doi.org/10.3390/ijerph15112406)
- Jacquez, G. M. (1996). A *k* nearest neighbour test for space-time interaction. *Statistics in Medicine*, 15(17–18), 1935–1949. doi: [10.1002/\(sici\)1097-0258\(19960930\)15:18%3C1935::aid-sim406%3E3.0.co;2-i](https://doi.org/10.1002/(sici)1097-0258(19960930)15:18%3C1935::aid-sim406%3E3.0.co;2-i)
- Johnson, S. D., Bowers, K. J., & Johnson, D. (2008). Stable and fluid differentiation of crime: Hotspots and identification. *Built Environment*, 34(1), 32–45. doi: [10.2148/benv.34.1.32](https://doi.org/10.2148/benv.34.1.32)
- Kelsall, J. E., & Diggle, P. J. (1995a). Kernel estimation of relative risk. *Bernoulli*, 1(1), 3–16. doi: [10.2307/3318678](https://doi.org/10.2307/3318678)
- Kelsall, J. E., & Diggle, P. J. (1995b). Non-parametric estimation of spatial variation in relative risk. *Statistics in Medicine*, 14, 2335–2342. doi: [10.1002/sim.4780142106](https://doi.org/10.1002/sim.4780142106)
- Kim, Y., & O’Kelly, M. (2008). A bootstrap based space-time surveillance model with an application to crime occurrences. *Journal of Geographical Systems*, 10(2), 141–165. doi: [10.1007/s10109-008-0058-4](https://doi.org/10.1007/s10109-008-0058-4)
- Knorr-Held, L. (2000). Bayesian modelling of inseparable space-time variation in disease risk. *Statistics in Medicine*, 19(17–18), 2555–2567. doi: [10.1002/1097-0258\(20000915/30\)19:17/18%3C2555::aid-sim587%3E3.0.co;2-#](https://doi.org/10.1002/1097-0258(20000915/30)19:17/18%3C2555::aid-sim587%3E3.0.co;2-#)
- Knox, E., & Bartlett, M. (1964). The detection of space-time interactions. *Applied Statistics*, 13(1), 25–30. doi: [10.2307/2985220](https://doi.org/10.2307/2985220)
- Kulldorff, M. (1997). A spatial scan statistic. *Communications in Statistics - Theory and Methods*, 26(6), 1481–1496. doi: [10.1080/03610929708831995](https://doi.org/10.1080/03610929708831995)
- Kulldorff, M. (2001). Prospective time periodic geographical disease surveillance using a scan statistic. *Journal of the Royal Statistical Society. Series A (statistics in Society)*, 164(1), 61–72. doi: [10.1111/1467-985X.00186](https://doi.org/10.1111/1467-985X.00186)
- Kulldorff, M., Heffernan, R., Hartman, J., Assunção, R., & Mostashari, F. (2005). A space-time permutation scan statistic for disease outbreak detection. *PLoS Medicine*, 2(3), 216–224. doi: [10.1371/journal.pmed.0020059](https://doi.org/10.1371/journal.pmed.0020059)
- Levine, N. (2010, July). *CrimeStat: A spatial statistics program for the analysis of crime incident locations (v 3.3)*. Washington, DC: National Institute of Justice. <https://www.nij.gov/topics/technology/maps/Pages/crimestat.aspx>
- Mantel, N. (1967). The detection of disease clustering and a generalized regression approach. *Cancer Research*, 27(2 Part 1), 209–220.
- Mburu, L. W., & Helbich, M. (2016). Crime risk estimation with a commuter-harmonized ambient population. *Annals of the American Association of Geographers*, 106(4), 804–818. doi: [10.1080/24694452.2016.1163252](https://doi.org/10.1080/24694452.2016.1163252)
- McLafferty, S., Williamson, D., & McGuire, P. G. (2000). Identifying crime hot spots using kernel smoothing. In V. Goldsmith, P. McGuire, J. Mollenkopf, & T. Ross (Eds.), *Analyzing crime patterns: Frontiers of practice* (pp. 77–87). Thousand Oaks, CA: SAGE. doi: [10.4135/9781452220369.n7](https://doi.org/10.4135/9781452220369.n7)
- Mohler, G. O., Short, M. B., Brantingham, P. J., Schoenberg, F. P., & Tita, G. E. (2011). Self-exciting point process modeling of crime. *Journal of the American Statistical Association*, 106(493), 100–108. doi: [10.1198/jasa.2011.ap09546](https://doi.org/10.1198/jasa.2011.ap09546)
- Nakaya, T., & Yano, K. (2010). Visualising crime clusters in a space-time cube: An exploratory data-analysis approach using space-time kernel density estimation and scan statistics. *Transactions in GIS*, 14(3), 223–239. doi: [10.1111/j.1467-9671.2010.01194.x](https://doi.org/10.1111/j.1467-9671.2010.01194.x)
- Nelson, A. L., Bromley, R. D. F., & Thomas, C. J. (2001). Identifying micro-spatial and temporal patterns of violent crime and disorder in the British city centre. *Applied Geography*, 21(3), 249–274. doi: [10.1016/s0143-6228\(01\)00008-x](https://doi.org/10.1016/s0143-6228(01)00008-x)
- Okabe, A., Satoh, T., & Sugihara, K. (2009). A kernel density estimation method for networks, its computational method and a GIS-based tool. *International Journal of Geographical Information Science*, 23(1), 7–32. doi: [10.1080/13658810802475491](https://doi.org/10.1080/13658810802475491)
- Paiva, T., Assunção, R., & Simões, T. (2015). Prospective space-time surveillance with cumulative surfaces for geographical identification of the emerging cluster. *Computational Statistics*, 30, 419–440. doi: [10.1007/s00180-014-0541-y](https://doi.org/10.1007/s00180-014-0541-y)
- Pei, T., Zhou, C., Zhu, A.-X., Li, B., & Qin, C. (2010). Windowed nearest neighbour method for mining spatio-temporal clusters in the presence of noise. *International Journal of Geographical Information Science*, 24(6), 925–948. doi: [10.1080/13658810903246155](https://doi.org/10.1080/13658810903246155)
- Porter, M. D., & Reich, B. J. (2012). Evaluating temporally weighted kernel density methods for predicting the next event location in a series. *Annals of GIS*, 18(3), 225–240. doi: [10.1080/19475683.2012.691904](https://doi.org/10.1080/19475683.2012.691904)
- Ratcliffe, J. H., & Rengert, G. F. (2008). Near-repeat patterns in Philadelphia shootings. *Security Journal*, 21(1–2), 58–76. doi: [10.1057/palgrave.sj.8350068](https://doi.org/10.1057/palgrave.sj.8350068)
- Rey, S. J., Mack, E. A., & Koschinsky, J. (2012). Exploratory space-time analysis of burglary patterns. *Journal of*

- Quantitative Criminology*, 28(3), 509–531. doi: [10.1007/s10940-011-9151-9](https://doi.org/10.1007/s10940-011-9151-9)
- Rogerson, P. A. (1997). Surveillance systems for monitoring the development of spatial patterns. *Statistics in Medicine*, 16, 2081–2093. doi: [10.1002/\(sici\)1097-0258\(19970930\)16:18%3C2081::aid-sim638%3E3.0.co;2-w](https://doi.org/10.1002/(sici)1097-0258(19970930)16:18%3C2081::aid-sim638%3E3.0.co;2-w)
- Rogerson, P. A. (2001). Monitoring point patterns for the development of space-time clusters. *Journal of the Royal Statistical Society: Series A (statistics in Society)*, 164(1), 87–96. doi: [10.1111/1467-985X.00188](https://doi.org/10.1111/1467-985X.00188)
- Rogerson, P. A., & Sun, Y. (2001). Spatial monitoring of geographic patterns: An application to crime analysis. *Computers, Environment and Urban Systems*, 25(6), 539–556. doi: [10.1016/S0198-9715\(00\)00030-2](https://doi.org/10.1016/S0198-9715(00)00030-2)
- Schoenberg, F. P. (2004). Testing separability in spatial-temporal marked point processes. *Biometrics*, 60(2), 471–481. doi: [10.1111/j.0006-341x.2004.00192.x](https://doi.org/10.1111/j.0006-341x.2004.00192.x)
- Scholz, R. W., & Lu, Y. (2014). Detection of dynamic activity patterns at a collective level from large-volume trajectory data. *International Journal of Geographical Information Science*, 28(5), 946–963. doi: [10.1080/13658816.2013.869819](https://doi.org/10.1080/13658816.2013.869819)
- Schubert, J. L. (2009). *Incorporating time and daily activities into an analysis of urban violent crime* (Doctoral Dissertation), University of Texas at Dallas.
- Scott, D. W. (1992). *Multivariate density estimation: Theory, practice, and visualization*. New York: Wiley.
- Sherman, L. W., Gartin, P. R., & Buerger, M. E. (1989). Hot spots of predatory crime: Routine activities and the criminology of place. *Criminology*, 27(1), 27–55. doi: [10.1111/j.1745-9125.1989.tb00862.x](https://doi.org/10.1111/j.1745-9125.1989.tb00862.x)
- Short, M. B., D’Orsogna, M. R., Brantingham, P. J., & Tita, G. E. (2009). Measuring and modeling repeat and near-repeat burglary effects. *Journal of Quantitative Criminology*, 25(3), 325–339. doi: [10.1007/s10940-009-9068-8](https://doi.org/10.1007/s10940-009-9068-8)
- Silverman, B. W. (1986). *Density estimation for statistics and data analysis*. New York: Chapman and Hall.
- Sonesson, C., & Bock, D. (2003). A review and discussion of prospective statistical surveillance in public health. *Royal Statistics Society*, 166(1), 5–21. doi: [10.1111/1467-985x.00256](https://doi.org/10.1111/1467-985x.00256)
- Tompson, L., & Townsley, M. (2010). Back to the future: Using space-time patterns to better predict the location of street crime. *International Journal of Police Science & Management*, 12(1), 23–40. doi: [10.1350/ijps.2010.12.1.148](https://doi.org/10.1350/ijps.2010.12.1.148)
- Waller, L. A., Zhu, L., Gotway, C. A., Gorman, D. M., & Gruenewald, P. J. (2007). Quantifying geographic variations in associations between alcohol distribution and violence: A comparison of geographically weighted regression and spatially varying coefficient models. *Stochastic Environmental Research and Risk Assessment*, 21(5), 573–588. doi: [10.1007/s00477-007-0139-9](https://doi.org/10.1007/s00477-007-0139-9)
- Wheeler, D. C. (2007). A comparison of spatial clustering and cluster detection techniques for childhood leukemia incidence in Ohio, 1996 – 2003. *International Journal of Health Geographics*, 6(1), 1–16. doi: [10.1186/1476-072x-6-13](https://doi.org/10.1186/1476-072x-6-13)
- Zhang, Z., Chen, D., Liu, W., Racine, J. S., Ong, S., Chen, Y., ... Jiang, Q. (2011). Nonparametric evaluation of dynamic disease risk: A spatio-temporal kernel approach. *PloS One*, 6(3), e17381. doi: [10.1371/journal.pone.0017381](https://doi.org/10.1371/journal.pone.0017381)
- Zhuang, J., Ogata, Y., & Vere-Jones, D. (2002). Stochastic declustering of space-time earthquake occurrences. *Journal of the American Statistical Association*, 97(458), 369–380. doi: [10.1198/016214502760046925](https://doi.org/10.1198/016214502760046925)